COHERENT PION PRODUCTION IN THE DELTA RESONANCE REGION*

P. OLTMANNS, B. KÖRFGEN, F. OSTERFELD

Institut für Kernphysik, KFA Jülich GmbH
52425 Jülich, Germany

AND

T. UDAGAWA

Department of Physics, University of Texas
Austin, Texas 78712, USA

(Received July 16, 1993)

Charge exchange reactions to the Δ-resonance region reveal a systematic downward energy shift of the Δ peak position in nuclei as compared to the proton target. Part of this shift is caused by a coherent medium effect on the spin-longitudinal response function. The coherent effect is produced by the attractive π exchange interaction between Δ-hole states in the medium. This shift is consistent with pion total cross section data. No shift is observed in the spin-transverse channel. In order to obtain more evidence for the coherent mode, exclusive cross section data of the $^{12}C(^3He, t\pi^+)^{12}C(g.s.)$ reaction are analyzed. We observe a strong energy shift in the coherent pion production cross section. The coherent pions have a peak energy of $E_\pi = 250$ MeV and a strongly forward peaked angular distribution, *i.e.* most of the pions can be detected in the direction of the momentum transfer $\vec{q}$. In addition it is shown that the quasi-free decay is suppressed in the energy domain where the decay nucleon has a small energy. At SATURNE a π^+ — coincidence spectrum was isolated where pions only inside a certain energy domain were taken into account. The features mentioned above prove that this spectrum consists to a great extent of coherent pions.

PACS numbers: 25.55. -e, 14.40. Aq, 13.75. Gx

---

* Presented at the Meson–Nucleus Interactions Conference, Cracow, Poland, May 14–19, 1993

1. Introduction

The (^{3}He,t) reactions at Laboratoire National Saturne in Paris [1, 2] have shown that there is a substantial downward shift in the excitation energy of the Δ resonance in nuclei compared to the Δ excitation in the proton target. This phenomenon is also found to persist, although to a variable extent, at higher bombarding energies [3] and also prevails in the (p,n) reaction at E=800 MeV [3] This shift of the Δ peak position has two different reasons: The first originates from the Fermi motion (binding) of the nucleons and of the Δ isobar in the nuclear mean field. This effect accounts for $\sim$ 40 MeV of the shift, leaving 30 MeV unexplained. This latter part of the shift is thought to be due to a nuclear medium correlation effect on the spin-longitudinal response function [4–7]. In particular, recent calculations of Delorme and Guichon [6] and Udagawa *et al.* [7] performed for finite nuclei consistently show that this second part of the shift is caused by the energy (ω)-dependent π-exchange interaction in the nuclear medium. The π-exchange provides a strongly attractive interaction between Δ-particle nucleon-hole (ΔN^{-1}) states in the spin-longitudinal ($\vec{S}\cdot\vec{q}\,\vec{T}$) channel leading to a lowering of the Δ mass in the nucleus. Other effects contributing to the shift come from Δ conversion processes, such as $\Delta + N \rightarrow N + N$ [6, 7] and from projectile excitation [8, 9].

The inclusive charge exchange cross sections contain information on both the spin-transverse (TR) and the spin-longitudinal (LO) nuclear response functions. Experimentally the two responses can be separated by measuring photon-nucleus and pion-nucleus scattering. The photon is a purely spin-transverse probe while the pion is a purely spin-longitudinal probe. In Figs 1(a) and 1(b) total cross sections for $\pi\,^{12}$C and $\gamma\,^{12}$C-scattering [10, 11] in the Δ resonance region are shown [12]. The data are compared to the free cross sections ($A \times \bar{\sigma}_{\gamma N}$) and ($A \times \bar{\sigma}_{\pi N}$), respectively, where A is the nuclear mass number and $\bar{\sigma} = {}^1/_2\,(\sigma_p + \sigma_n)$. In case of pion scattering a large energy shift is observed between the free Δ resonance and the Δ in the nucleus, while such a shift does not occur for photon scattering. This is so since the π-exchange potential couples only weakly to the TR channel. Since the (p,n) and (^{3}He,t) reactions are mixed LO - TR probes, the data of these reactions consist of two parts of opposite behaviour: the LO cross section which is shifted in energy and the TR cross section which is not shifted. In this paper we shall show that the coherent pion decay, as measured in the ^{12}C(^{3}He, $t\pi^+$)^{12}C(g.s.) reaction, can be a very sensitive probe on the LO response function. To demonstrate this we make use of a microscopic model which we used previously [7] for the description of Δ excitations in the (p,n) and $(^3\mathrm{He},t)$ inclusive reactions.

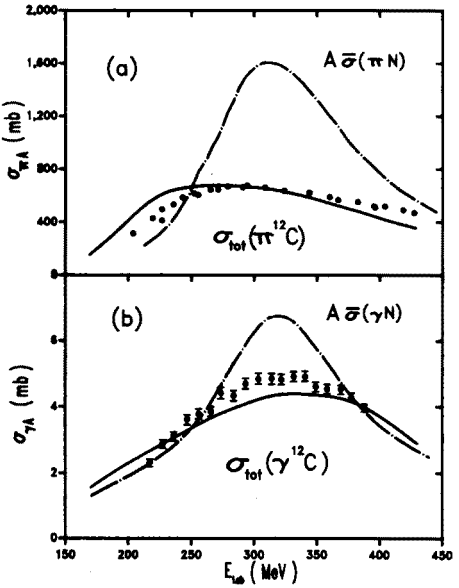

Fig. 1. The photon- and pion-nucleus total cross sections for ^{12}C. The data are taken from A. S. Carroll *et al.* [10] and H. Rost [11]. The dash-dotted curve in Fig.1(a) represents the incoherent sum of pion–nucleon total cross sections ($A \times \bar{\sigma}_{\pi N}$), and the dash-dotted curve in Fig. 1(b) represents the incoherent sum of photon–nucleon cross sections ($A \times \bar{\sigma}_{\gamma N}$), respectively. The solid curves represent microscopic calculations for the total cross sections [13].

2. The Model

2.1. Inclusive cross sections

Our approach is based on the isobar-hole model which has been successfully used in the description of pion-nucleus [14, 15] and photon-nucleus [16] scattering. In the isobar-hole model the Δ is assumed to move in a complex one-body potential. In addition, the Δ interacts with the residual nucleus B via a two-body interaction $V_{N\Delta,N\Delta}$. The wave function $|\psi\rangle$ describing the intermediate $(B + \Delta)$ system is then given by [7]

$$|\psi\rangle = G\,|\rho\rangle = \frac{1}{\omega + \frac{i\Gamma_\Delta}{2} - H_B - T_\Delta - U_\Delta - V_{N\Delta,N\Delta}}\,|\rho\rangle\,, \qquad (1)$$

where $|\rho\rangle$ is the doorway state excited initially by the reaction. This doorway state is characteristic for each reaction and is different for pion-, photon-, and charge exchange scattering. In Eq. (1) the Green's function G describes the propagation of the $(B + \Delta)$ system. $\Gamma_\Delta(\omega)$ is the energy

dependent free decay width of the Δ, H_B is the Hamiltonian of nucleus B, T_Δ and U_Δ are the kinetic energy operator and the Δ-nucleus one-body potential, respectively, and $V_{N\Delta,N\Delta}$ is the residual interaction describing the ΔN^{-1} correlations.

From Eq. (1) the inclusive cross section for the charge exchange reaction $A + a \to (B + \Delta) + b$ can be calculated as [7]

$$\frac{d^2\sigma}{dE_b d\Omega_b} = \frac{E_a E_b E_A E_{B+\Delta}}{(2\pi\hbar^2 c^2\sqrt{s})^2} \frac{p_b}{p_a} \frac{1}{\pi} \mathrm{Im}(-\langle \rho \mid \psi \rangle), \tag{2}$$

where E_i is the total energy of particle i ($i = A, B + \Delta, a, b$), p_a (p_b) is the momentum of particle a (b), and $\sqrt{s}$ is the total energy of all particles in the center of momentum system.

2.2. *Exclusive cross section for coherent pion decay*

Using the wave function $\mid \psi \rangle$ of Eq. (1) we can also calculate the transition amplitude T_{fi} for the coherent pion decay process $A+a \to (B+\Delta)+b \to A + \pi + b$. This amplitude is given by

$$T_{fi} = \sqrt{2E_{A'}2E_b}\langle \varphi_A, \phi(\vec{p}_\pi) \mid \frac{f_{\pi N\Delta}}{m_\pi} S \cdot \vec{\kappa}_\pi F(\kappa_\pi^2) T_\mu \mid \psi \rangle \sqrt{2E_A 2E_a}. \tag{3}$$

It describes the de-excitation of the $(B + \Delta)$ system to the target ground state $\mid \varphi_A \rangle$ by emission of a coherent pion of four-momentum $(E_\pi, \vec{p}_\pi)$. In Eq. (3) the $\pi N\Delta$ coupling is expressed in terms of the variables of the Δ rest frame (involving the spin- $(\vec{S})$ and isospin- $(\vec{T})$ transition operators and the relative pion-nucleon momentum $\vec{\kappa}_\pi$); $F(\kappa_\pi^2)$ is the $\pi N\Delta$ form factor. Note that the pion wave function $\phi(\vec{p}_\pi)$ in Eq. (3) is a plane wave. In spite of this fact, the pion distortion in the final channel is taken into account via the π-exchange interaction in $V_{N\Delta,N\Delta}$ which is included in Eq. (1). The threefold differential cross section for the $A(p, n\pi^+)A(\text{g.s.})$ reaction is then given by

$$\begin{aligned} \frac{d^3\sigma}{dE_b d\Omega_b d\Omega_\pi} = & \frac{1}{(2\pi)^5 16\sqrt{\lambda(s, M_a^2, M_A^2)}} \\ & \times \frac{p_b p_\pi}{\mid (E_A + \omega) + \frac{E_\pi}{p_\pi}(p_b \cos\theta_{b\pi} - p_a \cos\theta_{a\pi}) \mid} \\ & \times \frac{M_a}{E_a} \frac{M_b}{E_b} \overline{\sum} \mid T_{fi} \mid^2, \end{aligned} \tag{4}$$

where M_i stands for the mass of particle i ($i = A, B, a, b, \pi$) and $\overline{\Sigma}$ denotes the average over initial spin orientations and the sum over final spin orientations of both the projectile and target. The full three body kinematics in the final channel is included, *i.e.* $(E_a, \vec{p}_a) + (E_A, \vec{p}_A) = (E_b, \vec{p}_b) + (E_\pi, \vec{p}_\pi) + (E_{A'}, \vec{p}_{A'})$. The prime on A indicates that the nucleus A recoils in the π decay.

2.3. The $t_{NN,N\Delta}$ transition operator

In case of the charge exchange reaction A(a,b)B the doorway state entering Eq. (1) is explicitly given by

$$|\rho\rangle = (\chi_b^{(-)}\varphi_b \,|\, t_{NN,N\Delta} \,|\, \chi_a^{(+)}\varphi_a\varphi_A\rangle\,, \tag{5}$$

where $\chi_a^{(+)}$ and $\chi_b^{(-)}$ are the projectile distorted wave functions in the incident and exit channel, respectively, φ_a and φ_b are the intrinsic wave functions of a and b, and φ_A is the initial target wave function. The effective $NN \rightarrow N\Delta$ transition operator is denoted by $t_{NN,N\Delta}$. The following simple ansatz for $t_{NN,N\Delta}$ (in momentum representation) was made [7]

$$t_{NN,N\Delta} = t'_{N\Delta} J_{\pi N\Delta} \left(\frac{\Lambda'^2_\pi - m^2_\pi}{\Lambda'^2_\pi - t}\right)^2 \left[(\vec{\sigma}_1 \cdot \hat{q})(\vec{S}_2^\dagger \cdot \hat{q}) + (\vec{\sigma}_1 \times \hat{q}) \cdot (\vec{S}_2^\dagger \times \hat{q})\right] \vec{\tau}_1 \cdot \vec{T}_2^\dagger\,, \tag{6}$$

with $J_{\pi N\Delta} = 4\pi\hbar c f_{\pi NN} f_{\pi N\Delta}/m^2_\pi \approx 800$ MeV fm^3, $t'_{N\Delta} = 0.60$, and $\Lambda'_\pi = 650$ MeV. Despite of its simple structure, the $t_{NN,N\Delta}$ operator of Eq. (6) allows for an explanation of the $p(\vec{p}, \vec{n})\Delta^{++}$ data [17] and the $p(\vec{d}, 2p)\Delta^0$ data [18]. This concerns not only the cross section [7, 19], but also the spin observables [19–21].

2.4. The Δ–nucleus interaction

The Δ is assumed to move in a complex one-body potential. This potential is taken as a complex Woods-Saxon potential, $U_\Delta = V_\Delta + iW_\Delta$, with radius parameter $R = 1.1A^{1/3}$ fm and diffuseness $a = 0.53$ fm. The depths for the real and imaginary potential are $V_\Delta = -35$ MeV and $W_\Delta = -40$ MeV, respectively. Note that V_Δ is assumed to be the sum of the Δ-nucleus single particle potential (depth=-65 MeV) and of the real part of the Δ-spreading potential (strength=+30 MeV). W_Δ represents the imaginary part of the spreading potential [15]. The spreading potential accounts in a

phenomenological way for the increase of the Δ width in nuclei due to decay channels such as $\Delta N \to NN$.

The ΔN^{-1} interaction, $V_{N\Delta,N\Delta}$, is assumed to consist of the π and ρ exchange potentials with an additional short range interaction. In the momentum representation, $V_{N\Delta,N\Delta}$ may be given as a sum of LO and TR components

$$V_{N\Delta,N\Delta} = [V^L_{N\Delta,N\Delta}(\vec{S}_1\cdot\hat{q})(\vec{S}_2^{\dagger}\cdot\hat{q}) + V^T_{N\Delta,N\Delta}(\vec{S}_1\times\hat{q})\cdot(\vec{S}_2^{\dagger}\times\hat{q})]\vec{T}_1\cdot\vec{T}_2^{\dagger}\,, \quad (7)$$

where

$$V^L_{N\Delta,N\Delta} = 4\pi\hbar c\frac{f_\pi^2(t)}{m_\pi^2}\left[g'_{\Delta\Delta} + \frac{q^2}{t-m_\pi^2+i\epsilon} - \frac{2}{3}\frac{m_\pi^2}{f_\pi^2(t)}\frac{f_\rho^2(t)}{m_\rho^2}\frac{q^2}{t-m_\rho^2+i\epsilon}\right],$$

$$V^T_{N\Delta,N\Delta} = 4\pi\hbar c\frac{f_\pi^2(t)}{m_\pi^2}\left[g'_{\Delta\Delta} + \frac{1}{3}\frac{m_\pi^2}{f_\pi^2(t)}\frac{f_\rho^2(t)}{m_\rho^2}\frac{q^2}{t-m_\rho^2+i\epsilon}\right]. \quad (8)$$

In Eq. (8), the $f_i(t = \omega^2 - \vec{q}^{\,2})$ are the meson–baryon vertex form factors which we assume to be $f_i(t) = f_{iN\Delta}(\Lambda_i^2 - m_i^2)/(\Lambda_i^2 - t)$ $(i = \pi, \rho)$, and m_i and Λ_i are the mass and cut-off mass of the meson i, respectively. The various parameters are fixed as follows: $f^2_{\pi N\Delta} = 0.324$, $f^2_{\rho N\Delta} = 16.63$, $m_\pi = 0.14$ GeV, $m_\rho = 0.77$ GeV, $\Lambda_\pi = 1.20$ GeV, and $\Lambda_\rho = 2$ GeV. The Landau-Migdal parameter $g'_{\Delta\Delta}$ describes the short range correlations for $\Delta N^{-1} \to \Delta N^{-1}$ transitions. In the present calculations, we use the minimal $g'_{\Delta\Delta}$ that cancels out the δ-function like piece of the π-exchange potential. Then the Landau-Migdal parameter $g'_{\Delta\Delta} \approx 0.33$ (in units of $J_{\pi\Delta\Delta} = 4\pi\hbar c f_{\pi N\Delta} f_{\pi N\Delta}/m_\pi^2 \approx 1600$ MeV fm^3). Note that this parameter depends on the choice of U_Δ. Its accurate value is finally fixed from the requirement to reproduce the peak position of the Δ resonance in the medium.

3. Results and discussions

3.1. Inclusive (p,n) cross sections

In Fig. 2(a) we show the previously [7] calculated inclusive cross section for the 0-degree spectrum of the ^{12}C(p,n) reaction at 800 MeV incident energy in comparison to the experimental data [6]. The theoretical cross sections are calculated within the distorted wave impulse approximation (DWIA) using Eq. (2). The calculation underestimates the data by a factor of $N = 1.2$. This is due to the fact that the Δ-resonance is located on top of a large continuum (background). The background is the result of various

processes the importance of which varies with excitation energy: On the high energy side of the resonance ($\omega_L \geq 350$ MeV) the background is partly produced by projectile excitation where the proton is excited to a Δ^+ which subsequently decays into a $n + \pi^+$. Other contributions come from the Δ excitation in the nucleus which decays into a neutron and a pion where the decay neutron is detected (instead of the ejectile of the charge exchange reaction). These neutrons have a lower energy than the ejectile, because part of the energy for this mechanism is needed to create the decay pion. The neutrons should be smoothly distributed over a wide energy range. Both features can be seen in the experimental data. The cross section on the low energy side of the Δ resonance may be produced by nucleon-knockout, by multi-step processes, and by projectile excitation [22].

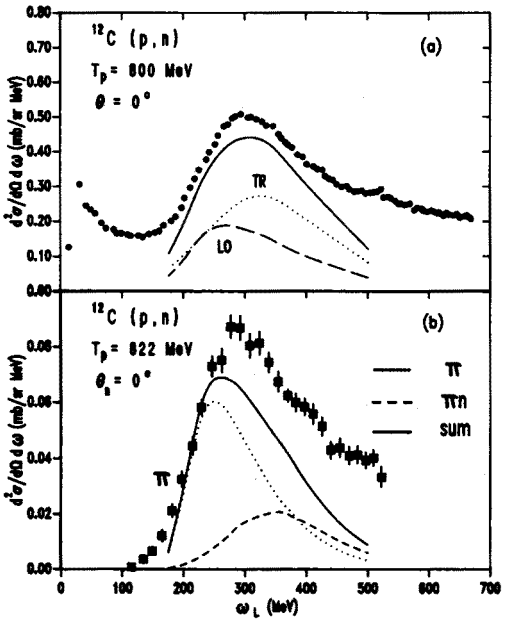

Fig. 2. Inclusive and exclusive $^{12}C(p, n)$ cross sections. (a) Calculated zero degree neutron spectra for the $^{12}C(p, n)$ reaction at $T_p = 800$ MeV in comparison with the experimental data of D.A. Lind *et al.* [3]. The spin-longitudinal and spin-transverse cross sections are shown separately. (b) Pion coincidence spectrum for the $^{12}C(p, n)$ reaction at $T_p = 822$ MeV. The data are taken from J. Chiba *et al.* [24]. The data are compared to the calculated zero degree coherent pion production cross section (dotted curve) and to the $\pi^+ n$ coincidence (dashed curve) cross section [23]. The sum of both cross sections is represented by the full curve.

In Fig. 2(a) we also show the correlated LO and TR cross sections separately. The peak position of the LO spectrum is lowered by $\sim$ 60 MeV

in energy in comparison with the TR spectrum. This is due to the attractive π-exchange interaction in the LO channel [6–8], as has been explained in detail in Ref. [7].

3.2. Coherent pion decay

In Fig. 2(b) we compare the $^{12}C(p, n\pi^+)^{12}C(g.s.)$ coincidence cross section (dotted curve) calculated [23] by means of Eq. (4) with the measured data of Chiba *et al.* [24]. The theoretical coincidence cross section peaks at an excitation energy of ω_L =250 MeV. This is in line with the peak position of the LO cross section in Fig. 2(a). The absolute magnitude of the calculated cross section has not been readjusted, *i.e.* no normalization factor N is included. Thus it is important that the coherent pion production cross section describes the slope of the data on the low-energy side correctly. In addition, the calculation shows that a large fraction of the experimentally observed pions are coherent pions. The cross section which is not described by the coherent pion production can arise from other processes, such as πn events or πp events where the proton has not been measured due to the acceptance of the detector (the detector FANCY at KEK accepts charged particles in the angular range $12° \leq \theta \leq 141°$ [24]). Other pions can come from projectile excitation events, *i.e.* where the projectile is excited to a Δ^+ which decays into $n + \pi^+$. In Fig. 2(b) we also show the theoretical cross section contribution from target $\pi^+ n$ events (dashed curve). This cross section has its peak at much higher excitation energy ($\omega_L \sim 350$ MeV) than the coherent pion production cross section. This added contribution leads to an improvement in the description of the data (full curve).

In Fig. 3 we compare the calculated angular distribution of the $(^3He, t\pi^+)$ reaction with the experimental differential cross section of this reaction as a function of the angle θ_π between the pion momentum $\hat{k}_\pi$ and the momentum transfer of the charge exchange reaction $\hat{q}$ taken at LNS [25]. In these data only events with triton angles between 2.5° and 3.5° and inside an energy window of 50 MeV around the ground state were considered. Therefore, these data can be only very carefully compared with our calculation. As the experimental data are given in arbitrary units, we have normalized our calculation so that the calculation agrees with the data in the forward direction, *i.e.* where the direction of the decay pion is parallel to the momentum transfer $\hat{q}$. We can see that these experimental data are in good agreement with the calculation at forward angles up to $\theta_\pi = 40°$. It should be noted that pions outside this energy window have a significantly different angular distribution (*i.e.* a rather flat one) than the ones inside.

The angular distribution resulting from the TR excitation of the nucleus has a characteristic shape with a minimum at $\theta_\pi = 0°$ and a maximum at $\theta_\pi \approx 30°$. This is very similar to the shape of the angular distributions

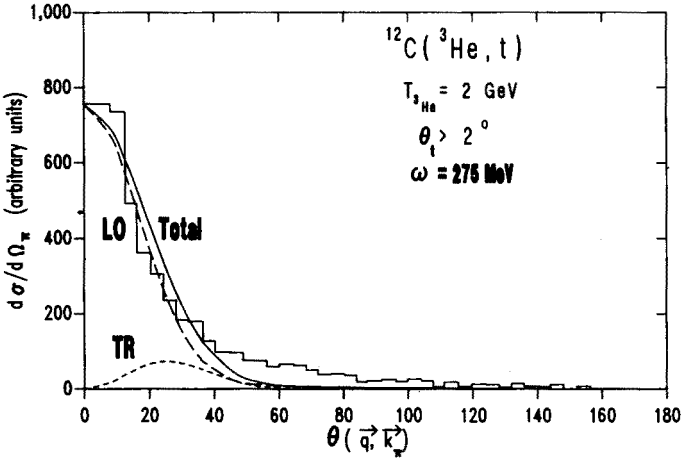

Fig. 3. Differential cross section of the $^{12}C(^3He,t\pi^+)$ reaction as function of the cosine of $\theta(\vec{q},\vec{k_\pi})$, which is the angle between the outgoing π^+ and the momentum transfer $\vec{q}$. The data are taken from T. Hennino *et al.* [25]. The theoretical curves are explained in the text.

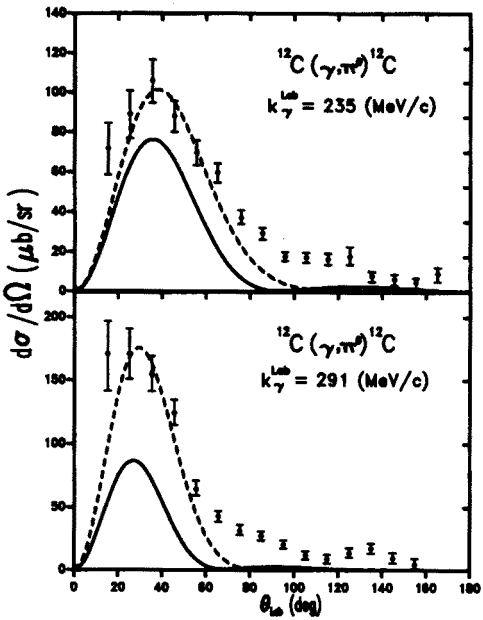

Fig. 4. Differential cross section for coherent π^0-photoproduction on ^{12}C at E_γ = 235 MeV and E_γ = 291 MeV. The data are taken from J. Arends *et al.* [26]. The full curves show the theoretical results with inclusion of $V_{N\Delta,N\Delta}$, the dashed curves without inclusion of $V_{N\Delta,N\Delta}$, respectively.

in coherent pion-photoproduction (Fig. 4). The reason for this is that the spin structure of the excitation ($\vec{S}^{\dagger} \times \vec{q}$) and de-excitation ($\vec{S} \cdot \vec{k}_{\pi}$) operators occurring in pion-photoproduction is exactly the same as that of the TR excitation of the nucleus by (p,n) reactions. The product of excitation and de-excitation operators is proportional to $\mid \vec{q} \times \vec{k}_{\pi} \mid = qk_{\pi} \sin\theta_{\pi}$ which vanishes for $\theta_{\pi}=0°$ and peaks for $\theta_{\pi}=90°$. However, an additional factor comes from the target transition matrix element in Eq. (3). This matrix element becomes the larger, the smaller the scattering angle θ_{π}. This is due to the dependence of the matrix element on the recoil momentum $\mid \vec{q} - \vec{p}_{\pi} \mid$ transferred to A' in the coherent π decay process. This recoil momentum is smallest for $\vec{q}$ parallel $\vec{p}_{\pi}$, making the matrix element largest for $\theta_{\pi}=0°$. Thus the observed TR angular distribution with its peak at $\theta_{\pi} = 30°$ is the result of two competing effects, one coming from the spin structure of the transition operators and the other coming from the target transition matrix element.

The LO angular distribution in Fig. 3 is very strongly forward peaked, *i.e.* most of the pions can be detected in the direction of the momentum transfer $\vec{q}$. This shows that there is an intimate relation between LO coherent pion production on the one hand and elastic pion–nucleus scattering on the other hand. In the former case an initially off-mass shell pion is converted into an on-mass shell pion by the multiple scattering in the nucleus. This conversion process is possible since the nucleus as a whole can pick up the recoil momentum needed to lift the pion on its mass shell. In the ^{12}C$(p,n\pi^{+})^{12}$C(g.s.) reaction the recoil momentum amounts to $\Delta q \approx 0.5$ fm^{-1} at $\omega_L = 250$ MeV corresponding to a recoil energy of $\Delta\omega_L \sim 0.5$ MeV for the ^{12}C nucleus.

In Fig. 4 we compare the calculated differential pion-photoproduction cross section at two different incident photon momenta with the data [26]. The full and dashed curves represent calculations with and without inclusion of the residual interaction $V_{N\Delta,N\Delta}$. One can recognize that both calculations describe the shape of the experimental angular distributions rather well. The calculations with inclusion of $V_{N\Delta,N\Delta}$, however, underestimate the absolute magnitude of the cross sections by a factor of ~ 2. The reason for this underestimate is twofold: on the one hand we have neglected various background contributions to the excitation process in the calculations. On the other hand the experimental data include besides the coherent pions also pions from other reaction processes where the final nucleus is left in an excited state. This is due to the experimental energy resolution which amounts only to ~ 15 MeV [26].

In Fig. 5 we compare the calculated excitation energy spectra for the ^{12}C$(\gamma,\pi^{0})^{12}$C(g.s.) reaction with the data [26]. One can notice that the calculations with and without inclusion of $V_{N\Delta,N\Delta}$ differ in magnitude and

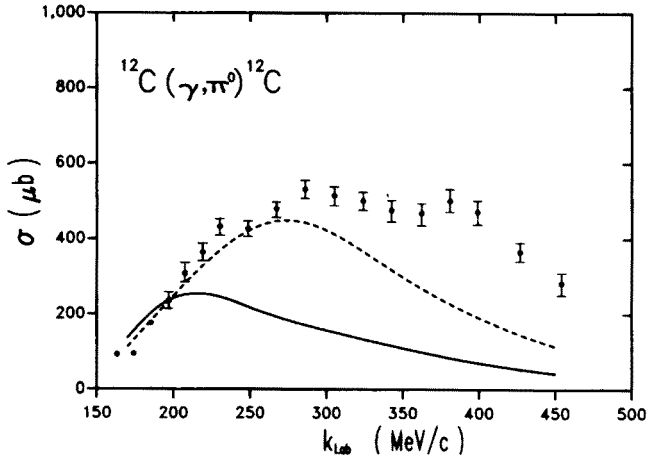

Fig. 5. Total cross section for coherent π^0-production on ^{12}C from J. Arends *et al.* [26] in comparison with the theoretical results. The calculations with and without inclusion of $V_{N\Delta,N\Delta}$ are shown by the full and dashed curves, respectively.

shape. The reduction in the calculation including the residual interaction (solid curve) relative to that without $V_{N\Delta,N\Delta}$ (dashed curve) is an effect of the pion distortion which is automatically included in the complete ΔN^{-1}-calculation. The peak position of the solid curve is shifted down in energy relative to the dashed curve by $\sim$ 80 MeV. This shift is an effect of the attractive residual interaction in the spin-longitudinal channel. Although the photon excites the nucleus spin-transversely, there is a mixing between the spin-transverse and spin-longitudinal channel due to the finiteness of the nucleus. The peak position of the coherent pion-photoproduction cross section is lowered in comparison to that of the $^{12}C(p,n\pi^+)^{12}C$(g.s.) reaction by $\sim$ 30 MeV (see Fig. 2(b)). This is so because the pion-photoproduction involves larger momentum transfers than the charge exchange reaction. Therefore the nuclear form factor suppresses the cross section in the former case.

3.3. Coherent vs incoherent pion decay

The main difficulty in analyzing the pion coincidence cross section is the distinction between coherent pions and pions originating from other processes. One very important non-coherent contribution to the pion spectrum is the quasi-free decay of a Δ into a neutron and a pion. Therefore this contribution has to be studied thoroughly.

The distortion of the decay protons and pions has been taken into account in our calculation by optical potentials fixed by elastic scattering. In Fig. 6 we have plotted the plane and distorted wave cross sections

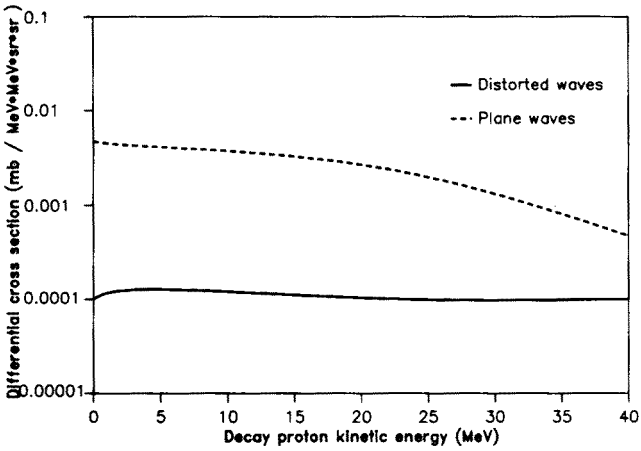

Fig. 6. Differential cross for quasi-free decay in the $^{12}C(p, np\pi^+)$-reaction. We have plotted our calculation for $(d^4\sigma)/(d\omega_L d\Omega_n d\Omega_\pi dE_p)$ as function of the decay proton energy E_p for low E_p ($E_p \leq 40$ MeV). The dashed curve represents the plane waves calculation, whereas the distorted waves calculation is shown by the solid curve.

$(d^3\sigma)/(d\omega_L d\Omega_n d\Omega_\pi)$ for $\omega_L = 250$ MeV and $\theta_n = \theta_\pi = 0°$ as function of the kinetic energy of the decay proton for small decay proton energies, *i.e.* the region where $p\pi$ events and coherent pion events cannot be disentangled easily. It can be seen that the contribution for very small decay proton energies is very strongly affected by the distortion. In order to compare with the coherent pion component we integrate this cross section over the decay proton kinetic energy up to $E_p = 30$ MeV.

We obtain the following result:

$$\frac{d^3\sigma}{d\omega_L d\Omega_n d\Omega_\pi}(\omega_L = 250\,\text{MeV},\ \theta_n = \theta_\pi = 0°)_{PW} = 0.022 \frac{\text{mb}}{\text{MeVsr}^2}, \quad (9)$$

$$\frac{d^3\sigma}{d\omega_L d\Omega_n d\Omega_\pi}(\omega_L = 250\,\text{MeV},\ \theta_n = \theta_\pi = 0°)_{DW} \leq 0.001 \frac{\text{mb}}{\text{MeVsr}^2}. \quad (10)$$

For this kinematic situation the corresponding cross section for the coherent pion component is

$$\frac{d^3\sigma}{d\omega_L d\Omega_n d\Omega_\pi}(\omega_L = 250\,\text{MeV},\ \theta_n = \theta_\pi = 0°) = 0.06 \frac{\text{mb}}{\text{MeVsr}^2}. \quad (11)$$

So the ratio of the coherent to the quasi-free component is at least equal to 60. As we use optical potentials from elastic scattering the actual distortion may be weaker than it is assumed in these calculations. Therefore we chose this rather high upper limit for the distorted waves calculation.

The fact that the $p\pi^+$ events where the decay proton energy is very small are suppressed can be understood considering the different mean free paths of protons and pions in nuclei. Protons have a very small mean free path at low energies whereas the pion mean free path has a broad minimum at high energies around 170 MeV which is about the energy of the decay pions in this energy domain. These mean free paths $l(E)$ can be calculated with the help of the pp and π^+p total cross sections as

$$l(E) = \frac{1}{\rho \times \sigma(E)}, \tag{12}$$

where ρ is the nuclear density and σ(E) the total cross section as function of the proton and pion energy E, respectively. Therefore we can conclude that inside the energy window set by the SATURNE experiment quasi-free decay is suppressed and does not make a significant contribution to the coincidence spectrum. This confirms the analysis that this spectrum consists to a great extent of coherent pions.

4. Conclusions

In summary, we have shown that the shift of the Δ-peak position observed in the (p,n)- and $(^3\mathrm{He},t)$-reactions at intermediate incident energies is due to the strongly attractive correlations in the isovector LO channel. The same shift is also observed in the pion–nucleus total cross section. The attraction comes from the energy-dependent π-exchange interaction in the medium. No significant energy shift is found in the TR channel. This is in agreement with what is observed in the electro-excitation of the Δ, *e.g.* in the photon–nucleus total cross section, as discussed in this paper.

Furthermore, we have shown that for charge exchange reactions the pion coincidence cross section is an excellent tool to study the LO response function. In the ^{12}C(^{3}He,$t\pi^+$)^{12}C(g.s.) reaction the peak position of the coherent pion component is significantly shifted towards lower excitation energies by the ΔN^{-1} correlations. In addition, it is shown that the pions are strongly forward (in the direction of $\hat{q}$) peaked. Both effects, the energy shift and the forward peaking of coherent pions, prove that the recent SATURNE experiment has indeed identified the coherent pion component in the ^{12}C(^{3}He,t) experiment.

This work is supported in part by the Studienstiftung des deutschen Volkes, by the Graduiertenkolleg "Die Erforschung subnuklearer Strukturen der Materie" at the University of Bonn and by the U.S. Department of Energy under Contract DE-FG05-84-ER40145.

REFERENCES

[1] For reviews on the experimental and theoretical situation of Δ's in nuclei see for example: C. Gaarde, *Ann. Rev. Nucl. Sci.* **41** 187 (1991); J. Delorme, P.A.M. Guichon, Proc. of the 10^{th} Biennale de Physique Nucleaire, p. C.4.1, Aussois 1989, Lycen 8906; F. Osterfeld, *Rev. Mod. Phys.* **64**, 491 (1992).

[2] D. Contardo *et al.*, *Phys. Lett.* **B168**, 331 (1986).

[3] D.A. Lind, *Can. J. Phys.* **65**, 637 (1987).

[4] G. Chanfray, M. Ericson, *Phys. Lett.* **B141**, 163 (1984).

[5] V.F. Dmitriev, T. Suzuki, *Nucl. Phys.* **A438**, 697 (1985).

[6] J. Delorme, P.A.M. Guichon, *Phys. Lett.* **B263**, 157 (1991).

[7] T. Udagawa, S. W. Hong, F. Osterfeld, *Phys. Lett.* **B245**, 1 (1990).

[8] E. Oset, E.Shiino, H.Toki, *Phys. Lett.* **B224**, 249 (1989).

[9] P.F. de Cordoba, E. Oset, *Nucl. Phys.* **A544**, 793 (1992).

[10] A.S. Carroll *et al.*, *Phys. Rev.* **C14**, 635 (1974).

[11] H. Rost, Bonn Report IR-80-10 (1980).

[12] T.E.O. Ericson, W. Weise, *Pions in Nuclei*, Oxford University Press, 1988.

[13] B. Körfgen, Berichte des Forschungszentrums Jülich, 2540 (1991).

[14] M. Hirata, J.H. Koch, F. Lenz, E.J. Moniz, *Phys. Lett.* **B70**, 281 (1977); M. Hirata, J.H. Koch, F. Lenz, E.J. Moniz, *Ann. Phys.* **120**, 205 (1979).

[15] Y. Horikawa, M. Thies, F. Lenz, *Nucl. Phys.* **A345**, 386 (1980).

[16] J.H. Koch, E.J. Moniz, N. Ohtsuka, *Ann. Phys.* **154**, 99 (1984).

[17] G. Glass *et al.*, *Phys. Lett.* **B129**, 27 (1983).

[18] C. Ellegaard *et al.*, *Phys. Lett.* **B231**, 365 (1989).

[19] P. Oltmanns, Berichte des Forschungszentrums Jülich, 2510 (1991).

[20] F. Osterfeld, B. Körfgen, P. Oltmanns, T. Udagawa, in: Proc. of the Workshop on Meson Production, Interaction and Decay, Cracow, Poland, May 6–11 1991, eds A. Magiera *et al.*, World Scientific, Singapore 1991, p. 116.

[21] T. Udagawa, F. Osterfeld, P. Oltmanns, Proc. of LAMPF Workshop on N-N and N-Nucleus Scattering, Los Alamos, New Mexico, to be published.

[22] P.F. de Córdoba *et al.*, Univ. Valencia preprint FTUV 92-50.

[23] P. Oltmanns, F. Osterfeld, T. Udagawa, *Phys. Lett.* **B299**, 194 (1993).

[24] J. Chiba *et al.*, *Phys. Rev. Lett.* **67**, 1982 (1991).

[25] T. Hennino *et al.*, *Phys. Lett.* **B303**, 236 (1993).

[26] J. Arends *et al.*, *Z. Phys.* **A311**, 367 (1983).